

# Design, simulation, fabrication, and characterization of a PMMA tunneling sensor based on hot embossing technique

J. Wang, T. Cui

452

**Abstract** Polymethyl methacrylate (PMMA) was chosen to fabricate highly sensitive tunneling sensors due to its extremely low cost and quick machining by hot embossing. The structure of an all-PMMA-based membrane vertical tunneling sensor platform was synthesized by ANSYS. The system characteristics and feedback system were evaluated with MatLab SimuLink. The first all-PMMA-based membrane tunneling transducers were produced by hot embossing replication with silicon masters. The fabricated tunneling sensors have presented a tunneling barrier height of 0.17 eV, a sensitivity of 26 V/g, and a dynamic range of 1.5 mg, which demonstrated competitive performances with lower cost, lighter weight, and easier fabrication processing.

## 1 Introduction

The applications of Microelectromechanical Systems (MEMS) have been focused on miniature, inexpensive, and batch-fabricated devices and systems. Several years after the advent of the first tunneling transducer [1], sensors with displacement resolution approaching  $10^{-5} \text{ nm}/\sqrt{\text{Hz}}$  were developed by Waltman [2] and Kenny [3], respectively. In electron tunneling transducers, sub-angstrom changes in displacement will induce measurable changes in tunneling current. This high sensitivity is independent of the lateral size of the electrodes because the tunneling current occurs between two metal atoms located at opposite electrode surfaces. Moreover, the tunneling current exponentially increases with displacement change by which tunneling sensors excel over most sensors such as piezoelectric, capacitive, piezoresistive, and interferential schemes.

An all-PMMA-based membrane vertical tunneling sensor platform was synthesized and fabricated using the hot embossing technique. The advantages of using PMMA are low cost (less than \$0.1 per square inch), low bonding temperature, and biocompatibility. Moreover, the hot embossing technique aiming at quick fabrication and high product rate was also employed. Due to the repeated usage of templates in hot embossing, the cost of mold fabrication can be almost neglected in the whole processing. The numerous replications of structures from template to PMMA make the hot embossing a real mass-production process. In this paper, the synthesis and system construction of the first all-PMMA-based tunneling sensor is used as an accelerometer. The sensor processing and measured characteristics are also reported.

## 2 Structure synthesis

Before fabrication, the structure parameters and mechanical properties were synthesized and simulated by ANSYS software. It is known that the ratio of spring constant  $k$  and proof mass  $m$  determines the sensitivity due to the relationship of

$$k/m = a/z \quad (1)$$

where  $a$  is the applied acceleration and  $z$  is the deflection displacement. In order to have a better sensitivity,  $k/m$  should be chosen smaller. On the other hand, the  $k/m$  ratio relates the natural frequency,  $\omega_n$ , of the membrane structure through

$$\omega_n = \sqrt{K/m} \quad (2)$$

Because the resonant frequency  $\omega_n$  constricts the natural response of applied force, it is better to have a larger  $k/m$  value. The compromise value of these two extremes was acquired by selecting the thicknesses and dimensions of the membrane and the proof mass with ANSYS simulation. As shown in Fig. 1, the ANSYS simulation tells that the maximum deflection exists at the center of the membrane, and the value of spring constant could be constructed through the applied force and the maximum deformation. Additionally, the proof mass was determined when the membrane structure was given. The whole simulation steps are:

1. Set a proper value of natural frequency,  $\omega_n$ .
2. Try to find several sets of ratios, which meet the need of  $k/m$ .
3. Figure out a possible sensitivity and test it.

Received: 30 April 2004 / Accepted: 17 June 2004

J. Wang, T. Cui  
Institute for Micromanufacturing,  
Louisiana Tech University,  
911 Hergot Avenue, Ruston, LA 71272, USA

T. Cui (✉)  
Department of Mechanical Engineering,  
University of Minnesota,  
111 Church Street SE, Minneapolis,  
MN 55455, USA  
Tel.: +612-626-1636  
Fax: +612-625-6019  
e-mail: tcui@me.umn.edu

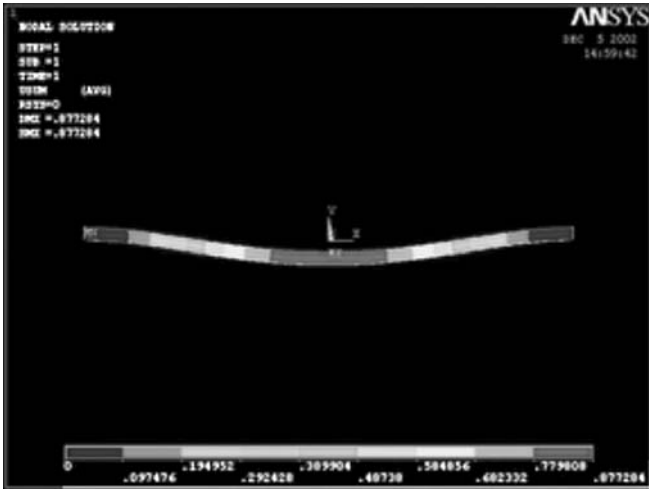


Fig. 1. Structure synthesis by ANSYS. Membrane deformation when the voltage is applied

4. Choose a proper thickness and a diameter of membrane to get the  $k$  value.
5. With synthesized structure and  $k/m$  aims, the proof mass was resolved.
6. Test the performance with ANSYS after structure synthesis. Make revision if any problem found.

The structures with 30  $\mu\text{m}$  in membrane thickness, 8 mm in diameter, and proof mass sizes of 100  $\mu\text{m} \times 100 \mu\text{m} \times 50 \mu\text{m}$ , were selected in this all-PMMA-based sensor.

### 3 Measurement system evaluation

After the final structures were synthesized by ANSYS, the measurement system was built by system analysis. The change of the tunneling tip to the proof mass distance,  $\Delta s$ , which was measured by Doppler Laser Vibrometer system as  $10^{-4}$  to  $10^{-2}$  nm [4], was rather small compared with the normal operation position of 1 nm. In this case, the tunneling current could be linearized and developed by the Taylor Series. Thus, the non-linear system can be changed into a linear system at wavelet analysis. The open- and closed-loop transfer function of whole system  $H_o$  and  $H$  were:

$$\begin{cases} H_o = H_c \cdot H' \\ H = \frac{H_o}{1 + FH_o} \end{cases} \quad (3)$$

where  $H_c$  was the control circuit transfer function,  $H'$  was the linear relation of the system, and  $F$  was the feedback factor. By choosing a designed control system, the accelerometer bandwidth was broadened and the damping was enhanced. The characteristics and feedback system could be evaluated with MatLab SimuLink.

Figure 2 shows the changes of normalized closed-loop transfer function when the control function magnitude increases. The closed loop property changed from an unstable, low damping system to a stable, damping optimized, and bandwidth broadened system. The system stability, root locus, step response, gain and phase margin, and pole-zero distribution can be plotted and surveyed.

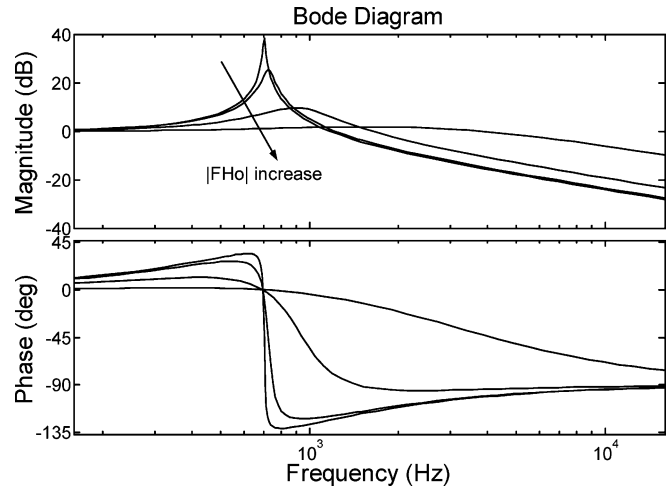


Fig. 2. After system is linearized, the closed-loop system transfer function changes when the control transfer function changes

With the designed control and feedback systems, a closed-loop system was stable on both the parameter disturbance and the frequency response. Compared with the real system at 50  $\text{ng}/\sqrt{\text{Hz}}$  noise level, the characteristics of tunneling accelerometers, such as the exponential relationship between the tunneling current and the displacement change, the time history record, the dynamics, and the frequency response were presented in another paper [5].

## 4 Fabrication process

### 4.1 Fabrication of silicon templates

The all-PMMA-based membrane tunneling transducers were produced by the hot embossing replication with silicon masters. The preparation of silicon templates for the hot embossing began with KOH wet etching because the pyramid like tunneling tip can be directly formed from anisotropic wet etching. The plasma deep etching, which produces high-aspect-ratio, smooth, and positively tapered sidewalls, was performed thereafter. The smooth and positive sidewall profiles are necessary, otherwise structure cracking at demolding phase would happen. Usually, a tunneling transducer includes different areas such as tunneling pyramid, which has a sharp tip to warrant tunneling current, and some grant blocks, which should have steep and high-aspect-ratio sidewalls. In the meantime, the height of the proof mass needs to be changed from chip to chip so that the parameters of transducers can be adjusted promptly. Consequently, it is hard to obtain single hot embossing templates only by conventional processes. The detailed description of combination method of KOH and plasma etchings for hot embossing was reported in another paper [6].

### 4.2 Structure replication by hot embossing

When using the hot embossing for structure replication, a polymer plate was laid onto the bottom heating plate of the

hot embossing machine, and the surrounding vacuum chamber was closed. Next, under vacuum, the heated mold insert was pressed into the softened PMMA. After subsequent cooling, demolding took place by removing the plastic part from the cavities. The demolding process was very important because all the parameters should be well controlled so that the microstructures were not destroyed by either the cracking of the mold or the friction of the sidewalls.

As shown in Fig. 3, the fabricated PMMA pyramids have smooth surfaces, sharp tip points, and steep edges, which can compete with any tunneling tip acquired by micromachining on silicon.

### 4.3

#### Packaging and assembly

The wire-electrode connection of the all-PMMA tunneling sensors was implemented by electrical conductive glue instead of wire bonding. The model of our electrical conductive glue was the Conductive Silver Epoxy Kit. The two-part silver epoxy was an electrically conductive silver filled epoxy adhesive, which was recommended for a wide range of electronic bonding and sealing applications. The bonding performed a combination of good mechanical and electrical properties. The two-part smooth paste formulation of refined pure silver and epoxy was free of solvents and copper or carbon additives. The PMMA structures were glued together, followed by fixing onto an 18-pin socket. The photographs of three packed sensors are shown in Fig. 4.

### 5

#### Measurement results

When the tunneling accelerometer operated at the open-loop status, the tunneling current was checked. A high dc voltage was applied on the deflection electrode, which set the gap between the tunneling tip and the counter electrode to a proper value. Next, an AC voltage with a frequency lower than the natural frequency,  $f_0$ , was applied on the deflection electrode. The inspired force produced a small vibration of the proof mass. An AC current,  $I_t$ , was induced on the tunneling tip, which had relation with both the high DC voltage and the AC deflection voltage. The measured

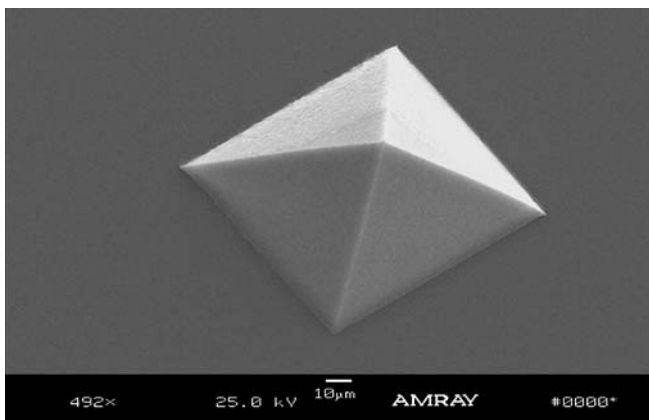


Fig. 3. SEM image of PMMA tunneling tip made by hot embossing replication

curve of the AC deflection voltage and the tunneling tip current is plotted in Fig. 5. The curve demonstrates that there is an exponential relationship between deflection voltage and tunneling current when the DC voltage is constant. This is the proof of the tunneling effect. According to the exponential relation of tunneling current:

$$I_t \propto V_B \cdot \exp(-\alpha\sqrt{\Phi}x) \quad (4)$$

where  $I_t$  is the tunneling current,  $V_B$  is the applied tunneling bias,  $\alpha$  is a constant approximately equal to  $1.025 \text{ \AA}^{-1} \text{ eV}^{-0.5}$ ,  $\phi$  is the effective tunneling barrier height or the effective work function of the electrode material, and  $x$  is the tunneling gap between two electrodes. The effective barrier height  $\Phi = 0.17 \text{ eV}$  was obtained, which is rather similar to the values in other groups [7, 8].

Sensitivity of the tunneling accelerometer describes the property of the ability to transfer the acceleration into the electrical signal. In an open-loop system, the sensitivity is determined by the  $k/m$  ratio. In a closed-loop system, however, the sensitivity of system is determined by the deep negative feedback factor, which was explained in [5]. Figure 6 illustrates the sensitivity measurement results. In this plot, the output voltages increase linearly with the acceleration. However, the sensitivity, which is  $20.6 \text{ V/g}$

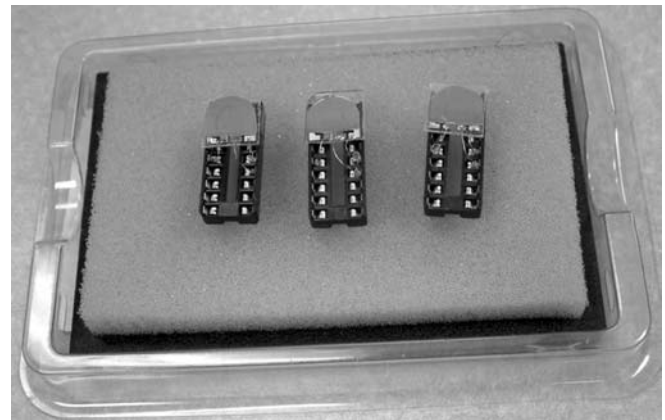


Fig. 4. Photographic pictures of constructed sensors after packaging and assembly

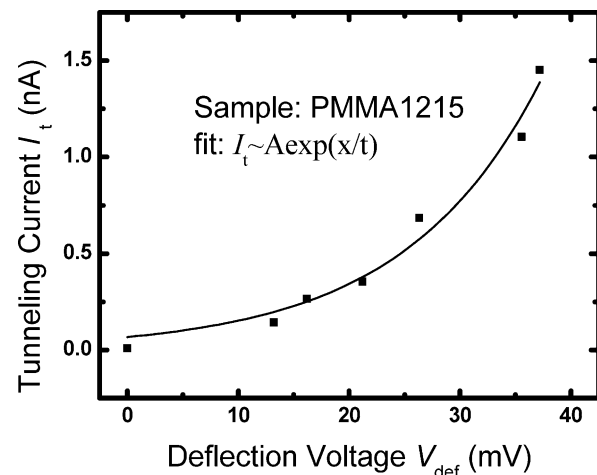


Fig. 5. Illustration of tunneling current changes versus applied voltages

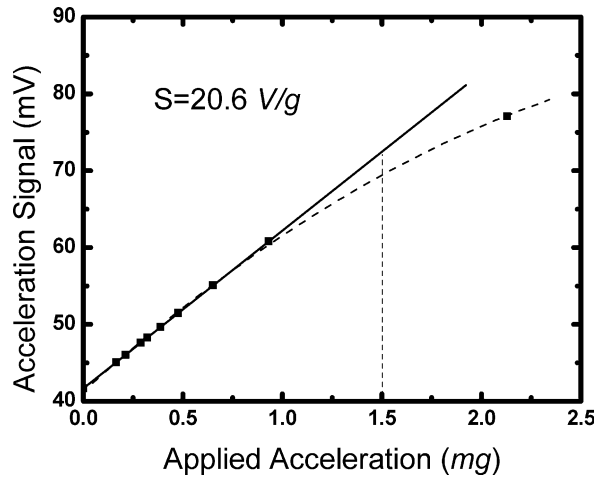


Fig. 6. The sensitivity of accelerometer plot. The linearity can be kept up to 1.5 mg

( $1\text{ g} = 9.8\text{ ms}^{-2}$ ), can only be kept linear lower than 1.5 mg, 10% distortion from linear relationship.

## 6 Conclusion

The first all-PMMA-based tunneling accelerometers were fabricated with the hot embossing replication. The structure parameters were obtained by ANSYS simulation, and the measurement system was established by MatLab Simulink. The exponential relationship between the tip currents and the applied deflection voltages proved the

tunneling effect, and thus presented the tunneling barrier height of 0.17 eV. The sensitivity is 26 V/g, which can be kept within the dynamic range of 1.5 mg. The all-PMMA-based tunneling sensors performed competitively with the advantages of lower cost, lighter weight, and easy fabrication processing.

## References

1. Quate CF (1988) Tunneling Accelerometer. *J Microscopy* 152: 73–76
2. Waltman SB; Kaiser WJ (1989) An electron tunneling sensor, *Sensors and Actuators, A: Physical*, 19: 201–210
3. Kenny TW; Waltman SB; Reynolds JK; Kaiser WJ (1991) Micro-machined silicon tunneling sensor for motion detection. *Appl Phys Lett* 58: 100–102
4. Liu CH; Grade JD; Barzilai AM; Reynolds JK; Partridge A; Rockstad HK; Kenny TW (1997) Characterization of a high-sensitivity micromachined tunneling accelerometer Source. *Int Conf Solid-State Sensors Actuators Proc* 1: 471–472
5. Wang J; Zhao Y; Cui T; Varahramyan K (2002) Synthesis of the modeling and control systems of a tunneling accelerometer using the MatLab simulation. *J Micromech Microeng* 12: 730–735
6. Wang J; Xue W; Cui T (2004) A Combinative Technique to Fabricate Hot Embossing Master for PMMA Tunneling Sensors. *Microsys Technol* 10: 329–333
7. Liu CH; Kenny TW (2001) A high-Precision, Wide-Bandwidth Micromachined Tunneling Accelerometer. *J Microelectromechanical Syst* 10: 425–433
8. Liu CH; Barzilai AM; Reynolds JK; Partridge A; Kenny TW; Garde JD; Rockstad HK (1998) Characterization of a High-Sensitivity Micromachined Tunneling Accelerometer with Micro-g Resolution. *J Microelectromechanical Syst* 7(2): 235–244